Eur. Phys. J. B **55**, 403–409 (2007)
DOI: 10.1140/epjb/e2007-00079-5

THE EUROPEAN PHYSICAL JOURNAL B

Second- and third-harmonic generations for a nondilute suspension of coated particles with radial dielectric anisotropy

L. Gao[a] and X.P. Yu

Department of Physics, Suzhou University, Suzhou 215006, P.R. China

Received 11 August 2006 / Received in final form 20 February 2007
Published online 22 March 2007 –

Abstract. We derive expressions for the effective nonlinear susceptibility tensors for both the second harmonic generation (SHG) and induced third harmonic generation (THG) of nonlinear composite materials, in which nondilute coated particles with radial dielectric anisotropy are randomly embedded in the linear host. Two types of coated particles are considered. The first is that the core possesses a second order nonlinear susceptibility and the shell is linear and radially anisotropic, while the second is that the core is linear with radial anisotropy and the shell has a second order nonlinear susceptibility. We observe greatly enhanced SHG and THG susceptibilities at several surface plasmon resonant frequencies. For the second model, due to the coating material being metallic, there exists two fundamental resonant frequencies ω_{c1} and ω_{c2}, whose difference $\omega_{c2}-\omega_{c1}$ is strongly dependent on the interfacial parameter and the radial dielectric anisotropy. Furthermore, in both systems, the adjustment of the dielectric anisotropy results in larger enhancement of both SHG and induced THG susceptibilities at surface plasmon resonant frequencies than the corresponding isotropic systems. Therefore, both the core-shell structure and the dielectric anisotropy play important roles in determining the nonlinear enhancement and the surface resonant frequencies.

PACS. 42.65.An Optical susceptibility, hyperpolarizability – 42.79.Ry Gradient-index (GRIN) devices – 72.20.Ht High-field and nonlinear effects – 77.84.Lf Composite materials

1 Introduction

Theoretical and experimental investigations on functional materials with large nonlinear optical properties and fast response time are of great interest in recent years for their potential applications in ultra-fast switching, optical signal processors, and bistable memory devices [1–3]. Composite materials may possess larger nonlinear optical properties such as third-order nonlinear susceptibility [4], second harmonic generation (SHG) susceptibility and third harmonic generation (THG) susceptibility [5] than those of their components, and even produce novel optical bistable and multi-stable properties [6,7] that none of the components have. These interesting physical properties of composite media are believed to result from the percolation mechanism [8] and the inhomogeneity of the local fields within the composites [9].

As we know, the enhancement of the local fields in composites can be realized by the choice of the microstructure and by the suitable adjustment of the physical parameters of the components. As for the microstructure, with the advancement in nanotechnology, it is possible to fabricate nanoparticles with specific microgeometry such as core-shell structures [10,11]. In this connection, large enhancement of optical nonlinear response was found in metal/semiconductor core-shell structures [12]. In addition, SHG susceptibility for a dilute suspension of core-shell nanoparticles was investigated [13], and optimal threshold intensity for optical bistability can be found in coated particles by tuning the core/shell thickness [14]. In a new report [15], the enhancement of effective third-order nonlinear susceptibility through the core-shell structures was observed experimentally. On the other hand, anisotropy in the components can also affect optical nonlinearity of composite media. For instance, composite systems containing carbon nanotube particles can achieve large optical third order nonlinearity due to the geometric anisotropy of nanotubes [16]. Moreover, anisotropy can be an intrinsic material property or can be induced by the application of fields [17].

In this paper, in order to obtain composite materials for a better nonlinear optical property, we hope to combine the special optical properties of core-shell structure and intrinsic material anisotropy in a composite system, in which the coated inclusions with second order nonlinear susceptibility are randomly embedded in a linear dielectric host. For coated inclusions, we consider two simple cases, one is the core being second order nonlinear and the shell being dielectric anisotropic (model A), while the second is the core being anisotropic and the shell being nonlinear (model B). To one's interest, the dielectric tensor will be

[a] e-mail: leigao@suda.edu.cn

assumed to be radially anisotropic, i.e., it is diagonal in spherical coordinates with a value ϵ_r in the radial direction and ϵ_t in the tangential directions. Such an anisotropy can be easily established from a problem of graphitic multishells [18], spherically stratified medium [19], and indeed found in cell membranes containing mobile charges [20]. In addition to the consideration of both the coated microstructures and the physical anisotropy, we further consider the coated inclusions to be in nondilute case instead of the dilute limit [13]. As a result, the electrostatic interactions among nonlinear coated inclusions must be taken into account. We would like to investigate the effective nonlinear susceptibility for second harmonic generation (SHG) and induced third harmonic generation (THG) of the composite system. For this purpose, we adopted general expressions for SHG and THG of composite materials, derived by Hui et al. [21,22]. Actually, these analytical expressions were recently applied to random composite materials of graded spherical particles [23] and compositionally graded films [24].

Our paper is organized as follows. In Section 2, we describe the model and outline briefly the effective SHG and induced THG susceptibilities of the composites. In Section 3, the analytical expressions for the effective SHG and induced THG susceptibilities for model A are derived and the numerical results are given. In Section 4, we study the case for model B. This paper ends with a discussion and conclusion in Section 5.

2 effective nonlinear susceptibilities for SHG and THG

We consider a macroscopically inhomogeneous material containing a nondilute suspension of nonlinear coated particles embedded in a linear host with the dielectric constant ϵ_m. The core (or the shell) is assumed to be second-order nonlinear due to the fact that the inversion symmetry is broken at the surface [25,26]. The local constitutive relation between the displacement field $\mathbf{D}$ and the electric field $\mathbf{E}$ of the core and the shell in the static case is

$$D_i^\alpha = \sum_{j=x}^{z} \epsilon_{ij}^\alpha E_j + \sum_{j,k=x}^{z} d_{ijk}^\alpha E_j E_k \qquad (i = x, y, z \text{and} \quad \alpha = c, s) \quad (1)$$

where D_i and E_i are the ith component of $\mathbf{D}$ and $\mathbf{E}$, and d_{ijk}^α is the components of second order nonlinear susceptibility tensor of the core or the shell.

When we apply a monochromatic external field $\mathbf{E}_0(t) = E_{0,z}(\omega)e^{-i\omega t} + c.c$ along z-axis to the composite system, the local potentials and fields will be generated at all harmonic frequencies due to the quadratic nonlinearity of the components inside the composite. Thus at finite frequencies, the constitutive relation in the particles will be [22]

$$D_i^\alpha = \sum_{n=-\infty}^{\infty} D_i^\alpha(n\omega)e^{-in\omega t} \quad (2)$$

with

$$D_i^\alpha(n\omega) = (\epsilon^\alpha)^{(n\omega)} E_i(n\omega) + \sum_{j,k=x}^{z} \sum_{m=-\infty}^{\infty} (d_{ijk}^\alpha)^{[(n-m)\omega, m\omega]} E_j[(n-m)\omega] E_k(m\omega),$$

where $(\epsilon^\alpha)^{(n\omega)}$ denotes the frequency dependent linear dielectric constant in component α, while $(d_{ijk}^\alpha)^{[(n-m)\omega,m\omega]}$ represent the second order nonlinear susceptibilities.

We aim at studying the effective second and third harmonic susceptibilities of the composite system. The effective nonlinear SHG susceptibility $d_{e,ijk}^{(\omega,\omega)}$ can be written in the form [21]

$$d_{e,ijk}^{(\omega,\omega)} = \sum_{\alpha=c}^{s} f_\alpha \left\langle K_{il}^{2\omega} (d_{lmn}^\alpha)^{(\omega,\omega)} K_{jm}^\omega K_{kl}^\omega \right\rangle_\alpha \quad (3)$$

where $\langle ... \rangle$ stands for the spatial average of ..., f_α is the volume fraction of component α, and $K_{il}^\omega \equiv E_l(\omega)/E_{0,i}(\omega)$ is the local field factor giving the lth Cartesian component of linear electric field inside the particles when the external field E_0 is applied along the ith direction at frequency ω. Here we would like to mention that repeated indices such as l, m, n in equation (3) should be summed over.

For the effective THG susceptibility $\chi_{e,ijkl}^{(\omega,\omega,\omega)}$, one has [22,23]

$$\chi_{e,ijkl}^{(\omega,\omega,\omega)} = \sum_{\alpha=c}^{s} f_\alpha \left\langle 2K_{im}^{3\omega} (d_{mnp}^\alpha)^{(\omega,2\omega)} \cdot \frac{K_{rn}^{2\omega} - I_{rn}}{\delta(\epsilon^\alpha)^{(2\omega)}} \cdot (d_{rst}^\alpha)^{(\omega,\omega)} K_{js}^\omega K_{kt}^\omega K_{lp}^\omega \right\rangle_\alpha, \quad (4)$$

from equation (4), we observe that although the component possesses the second-order nonlinear response, the whole system shall induce the effective third-order nonlinear susceptibility.

In what follows, we shall study the effective SHG susceptibility and the induced THG susceptibility for two kind of models.

3 SHG and THG susceptibilities for model A

We consider that a nondilute suspension of nonlinear coated particles randomly embedded in a linear host. The coated spheres consist of nonlinear core of radius r_0 and the linear shell of radius $R > r_0$ with radial dielectric anisotropy (Model A). The nonlinear core has the linear dielectric constant ϵ_c and second-order susceptibility tensor $\overleftrightarrow{d}_c$. And the shell is linear and radially anisotropic with $\overleftrightarrow{\epsilon}_s = \epsilon_{sr}\mathbf{e}_r\mathbf{e}_r + \epsilon_{st}(\mathbf{e}_\theta\mathbf{e}_\theta + \mathbf{e}_\varphi\mathbf{e}_\varphi)$.

When a monochromatic external field is applied, say along z-axis, we want to solve the potential function in the core, the shell and the host. Since the coated inclusions under consideration are in nondilute, the electrostatic dipolar interaction among the coated inclusions

should be taken into account. In this regard, the local electric fields in the system are affected not by $\mathbf{E}_0$, but rather by the Lorentz field $\mathbf{E}_L$. The solution is as follows,

$$\begin{cases} \phi_c = -A_1 E_L r\cos\theta & r < r_0 \\ \phi_s = -E_L\left(B_1 r^{\nu_1} - \frac{C_1}{r^{\nu_1+1}}\right)\cos\theta & r_0 < r < R \\ \phi_m = -E_L\left(r - \frac{D_1 R^3}{r^2}\right)\cos\theta & r > R \end{cases} \quad (5)$$

where

$$A_1 = \frac{3\epsilon_m\epsilon_{sr}(2\nu_1+1)\lambda^{(\nu_1-1)/3}}{Q_1}$$

$$\text{and} \quad B_1 = \frac{3\epsilon_m[\epsilon_{sr}(1+\nu_1)+\epsilon_c]R^{1-\nu_1}}{Q_1}$$

$$C_1 = \frac{-3\epsilon_m\lambda^{(2\nu_1+1)/3}(\epsilon_{sr}\nu_1-\epsilon_c)R^{\nu_1+2}}{Q_1}$$

$$\text{and} \quad D_1 = \frac{P_1}{Q_1},$$

with interfacial parameter $\lambda = (r_0/R)^3$ and

$$\nu_1 = \frac{1}{2}\left(\sqrt{1+8\epsilon_{st}/\epsilon_{sr}}-1\right)$$

$$P_1 = (\epsilon_{sr}\nu_1-\epsilon_m)[\epsilon_c+(1+\nu_1)\epsilon_{sr}] + \lambda^{(2\nu_1+1)/3}[\epsilon_m+(1+\nu_1)\epsilon_{sr}](\epsilon_c-\epsilon_{sr}\nu_1)$$

$$Q_1 = [\epsilon_{sr}(1+\nu_1)+\epsilon_c](\epsilon_{sr}\nu_1+2\epsilon_m) + \lambda^{(2\nu_1+1)/3}[2\epsilon_m-\epsilon_{sr}(1+\nu_1)](\epsilon_{sr}\nu_1-\epsilon_c).$$

The averaged field over the entire system, inside and outside the inclusions, must be equal to $\mathbf{E}_0$, that is

$$f\langle\mathbf{E}_c\rangle + \left(\frac{f}{\lambda}-f\right)\langle\mathbf{E}_s\rangle + \left(1-\frac{f}{\lambda}\right)\mathbf{E}_L = \mathbf{E}_0, \quad (6)$$

where f is the volume fraction of the core.

To establish the relation between $\mathbf{E}_L$ and $\mathbf{E}_0$, according to equation (6), we need to calculate the average fields in the nonlinear core and anisotropic shell. Especially, the local electric field in the shell is derived to be,

$$\mathbf{E}_s = \left[E_L B_1(\nu_1-1)r^{\nu_1-1} + E_L C_1(\nu_1+2)\frac{1}{r^{\nu_1+2}}\right] \times \sin\theta\cos\theta(\cos\varphi\mathbf{e}_x+\sin\varphi\mathbf{e}_y) + \left\{\left[E_L B_1\nu_1 r^{\nu_1-1} + E_L(\nu_1+1)\frac{C_1}{r^{\nu_1+2}}\right]\cos^2\theta + \left[E_L B_1 r^{\nu_1-1} - E_L\frac{C_1}{r^{\nu_1+2}}\right]\sin^2\theta\right\}\mathbf{e}_z,$$

and hence

$$\langle\mathbf{E}_s\rangle = \left[E_L B_1\left(\frac{R^{\nu_1+2}-r_0^{\nu_1+2}}{R^3-r_0^3}\right) - E_L C_1\left(\frac{R^{1-\nu_1}-r_0^{1-\nu_1}}{R^3-r_0^3}\right)\right]\mathbf{e}_z.$$

Then we can obtain the relation between $\mathbf{E}_0$ and $\mathbf{E}_L$,

$$\mathbf{E}_L = \frac{Q_1}{Q_1-\frac{f}{\lambda}P_1}\mathbf{E}_0. \quad (7)$$

For convenience, we suppose $d_{lll} \neq 0$ for $l = x, y, z$ only. In this case, the local field factor K_{il}^{ω} is nonzero only for $i = l$. When we apply the general expressions for SHG and THG [see Eqs. (3) and (4)] to the present model, we only get the surviving effective SHG susceptibility d_{zzz}^e and the THG susceptibility χ_{zzzz}^e, which are written as

$$\frac{d_{zzz}^e}{f d_{zzz}^{(\omega,\omega)}} = \left(\frac{A_1 Q_1}{Q_1-\frac{f}{\lambda}P_1}\right)_{2\omega}\left(\frac{A_1 Q_1}{Q_1-\frac{f}{\lambda}P_1}\right)_{\omega}^2, \quad (8)$$

and

$$\frac{\chi_{zzzz}^e}{f d_{zzz}^{(\omega,2\omega)} d_{zzz}^{(\omega,\omega)}} = \frac{2}{\epsilon_c^{2\omega}-\epsilon_{e1}^{2\omega}}\left(\frac{A_1 Q_1}{Q_1-\frac{f}{\lambda}P_1}\right)_{3\omega} \times\left[\left(\frac{A_1 Q_1}{Q_1-\frac{f}{\lambda}P_1}\right)_{2\omega}-1\right]\left(\frac{A_1 Q_1}{Q_1-\frac{f}{\lambda}P_1}\right)_{\omega}^3, \quad (9)$$

where

$$\epsilon_{e1}^{2\omega} = \left[\epsilon_m + 3\frac{f}{\lambda}\epsilon_m\frac{P_1}{Q_1-\frac{f}{\lambda}P_1}\right]_{2\omega}. \quad (10)$$

As numerical examples, we consider the core to be a Drude metal, which has a dielectric constant of the form

$$\epsilon_c(\omega) = 1-\frac{\omega_p^2}{\omega^2+i\omega/\tau},$$

with ω_p being the plasma frequency and τ the relaxation time . We take $\omega_p = 2.28\times10^{16}$ s^{-1} and $\tau = 6.9\times10^{-15}$ s [13], The anisotropic shell is assumed to have a frequency-independent radial dielectric constant $\epsilon_{sr} = 2.52$, while the host medium also has a frequency-independent dielectric constant $\epsilon_m = 1.76$. These values are typical of nonconducting materials.

Figure 1 shows the effective nonlinear susceptibility for SHG $d_{zzz}^e/f d_{zzz}^{(\omega,\omega)}$ as a function of frequency ω/ω_p for various interfacial parameter λ and for different ratios of tangential dielectric constant ϵ_{st} to radial dielectric constant ϵ_{sr}. Since SHG susceptibility intrinsically involves two different frequencies, there are two enhancement peaks in d_{zzz}^e, one located at the surface plasmon frequency ω_c while the other located at the half of ω_c as expected. Moreover, large enhancement of SHG susceptibility is found to be the order of 10^4 at ω_c. To one's interest, when the ratio of tangential dielectric constant to radial dielectric constant decreases, the enhancement peaks are enlarged with the locations shifted to high frequency region. This indicates that the radial dielectric anisotropy is helpful to realize the enhancement of SHG susceptibility and change the surface plasmon frequencies.

Figure 2 shows the induced nonlinear susceptibility of third harmonic generations (THG susceptibility)

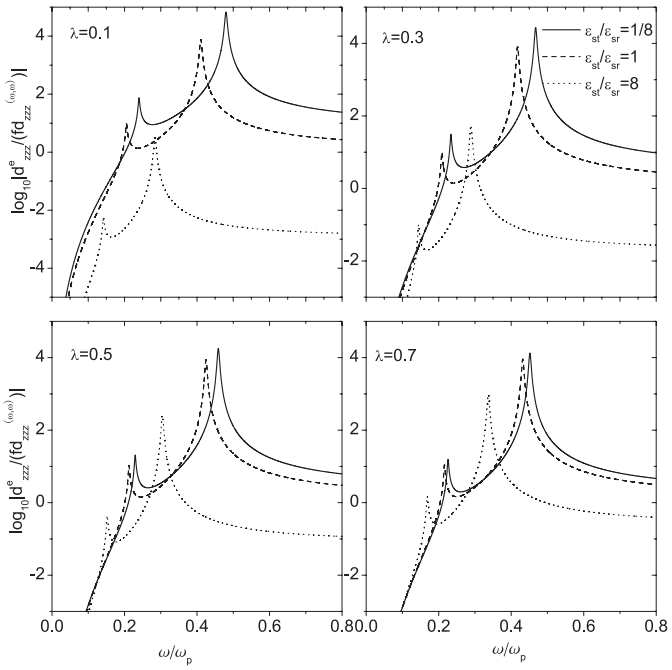

Fig. 1. For model A, the enhancement of effective SHG susceptibility $|d^e_{zzz}/(fd^{(\omega,\omega)}_{zzz})|$ against the normalized incident angular frequency ω/ω_p for the volume fraction of coated particles $f/\lambda = 0.1$.

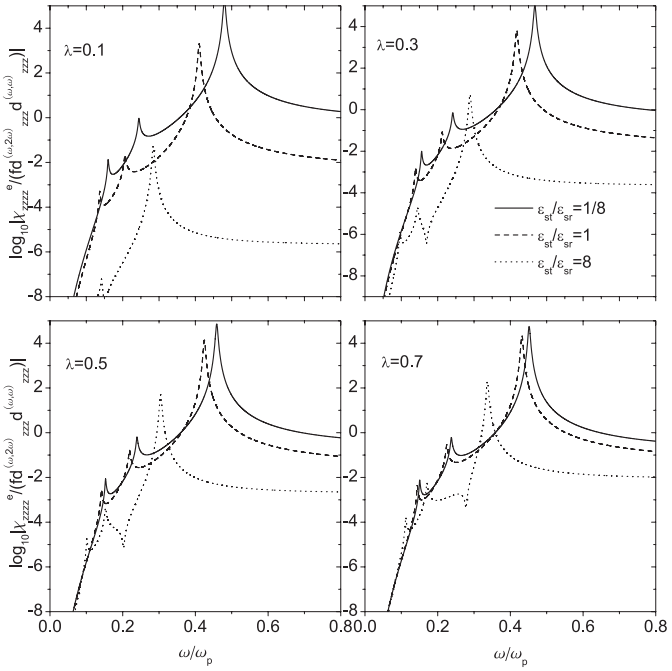

Fig. 2. Same as Figure 1, but for the induced THG susceptibility $|\chi^e_{zzzz}/(fd^{(\omega,2\omega)}_{zzz}d^{(\omega,\omega)}_{zzz})|$.

$\chi^e_{zzzz}/fd^{(\omega,2\omega)}_{zzz}d^{(\omega,\omega)}_{zzz}$. For THG susceptibility, there exist three enhancement peaks, with the predominant one located at the resonant frequency ω_c. The reason is that the present nonlinear optical process involves the effect of first forming a 2ω component and then combining the 2ω component with a ω component to give a 3ω component. On the other hand, the enhancement of THG susceptibility is found to be the order of 10^5. As far as the effect of dielectric anisotropy is concerned, the behavior for THG susceptibility is quite similar as that for SHG susceptibility in Figure 1. That is, the large effective THG susceptibility can be indeed achieved at the high frequency region when the ratio of tangential dielectric constant ϵ_{st} to radial dielectric constant ϵ_{sr} is small. Therefore, the dielectric anisotropy plays an important role in determining the magnitude and the resonant frequencies of the SHG and THG susceptibilities.

4 SHG and THG susceptibilities for Model B

Model B is similar as Model A, except that the core of the coated spheres is linear and radially anisotropic with $\overleftrightarrow{\epsilon}_c = \epsilon_{cr}\mathbf{e}_r\mathbf{e}_r + \epsilon_{ct}(\mathbf{e}_\theta\mathbf{e}_\theta + \mathbf{e}_\varphi\mathbf{e}_\varphi)$, while the shell is nonlinear with linear dielectric constant ϵ_s, and second order susceptibility tensor $\overleftrightarrow{d}_s$. To have a unique defined dielectric constant for the core, let the origin at the core be surrounded by a small sphere of isotropic dielectric constant ϵ_{cr} [19].

For such a model, we express the solutions of the potential function in the core, the shell and the host as,

$$\begin{cases} \phi_c = -A_2 E_L r^{\nu_2}\cos\theta & r < r_0 \\ \phi_s = -E_L\left(B_2 r - \frac{C_2 r_0^3}{r^2}\right)\cos\theta & r_0 < r < R \\ \phi_m = -E_L\left(r - \frac{D_2 R^3}{r^2}\right)\cos\theta & r > R \end{cases} \tag{11}$$

where

$$A_2 = \frac{9\epsilon_m\epsilon_s r_0^{1-\nu_2}}{Q_2} \quad \text{and} \quad B_2 = \frac{3\epsilon_m\left(2\epsilon_s + \epsilon_{cr}\nu_2\right)}{Q_2}$$
$$C_2 = \frac{3\epsilon_m\left(\epsilon_{cr}\nu_2 - \epsilon_s\right)}{Q_2} \quad \text{and} \quad D_2 = \frac{P_2}{Q_2},$$

with

$$\nu_2 = \frac{1}{2}\left(\sqrt{1 + 8\epsilon_{ct}/\epsilon_{cr}} - 1\right),$$
$$P_2 = (2\epsilon_s + \epsilon_{cr}\nu_2)(\epsilon_s - \epsilon_m) + \lambda(\epsilon_{cr}\nu_2 - \epsilon_s)(2\epsilon_s + \epsilon_m),$$
$$Q_2 = (\epsilon_s + 2\epsilon_m)(2\epsilon_s + \epsilon_{cr}\nu_2) + 2\lambda(\epsilon_s - \epsilon_m)(\epsilon_{cr}\nu_2 - \epsilon_s).$$

Then, the local fields in the core and the shell are found to be

$$\mathbf{E}_c = A_2 E_L r^{\nu_2 - 1}\left[(\nu_2 - 1)\sin\theta\cos\theta(\cos\varphi\mathbf{e}_x + \sin\varphi\mathbf{e}_y) + (\nu_2\cos^2\theta + \sin^2\theta)\mathbf{e}_z\right],$$
$$\mathbf{E}_s = E_L\left\{\frac{3C_2 r_0^3}{r^3}\cos\theta\sin\theta(\cos\varphi\mathbf{e}_x + \sin\varphi\mathbf{e}_y) + \left[B_2 + \frac{C_2 r_0^3}{r^3}(2\cos^2\theta - \sin^2\theta)\right]\mathbf{e}_z\right\}, \tag{12}$$

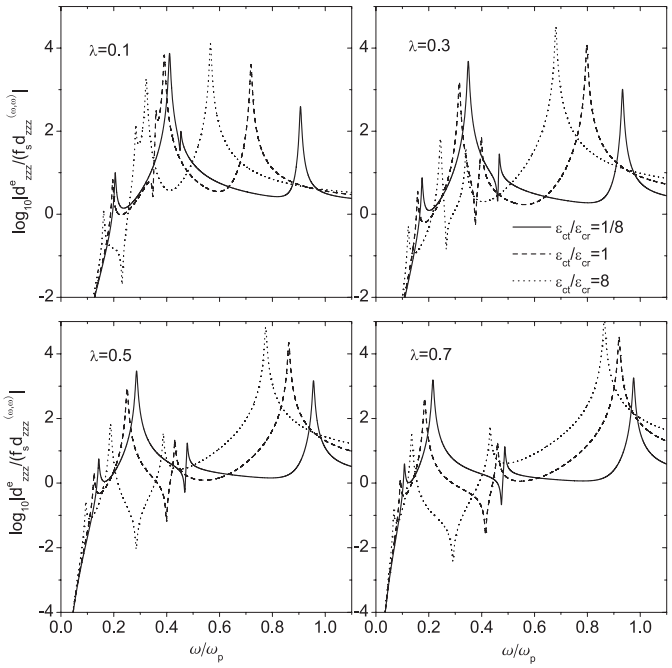

Fig. 3. Same as Figure 1, but for the enhancement of effective SHG susceptibility $|d_e \equiv d^e_{zzz}/(f_s d^{(\omega,\omega)}_{zzz})|$ with $f_s \equiv (f/\lambda - f)$ for model B.

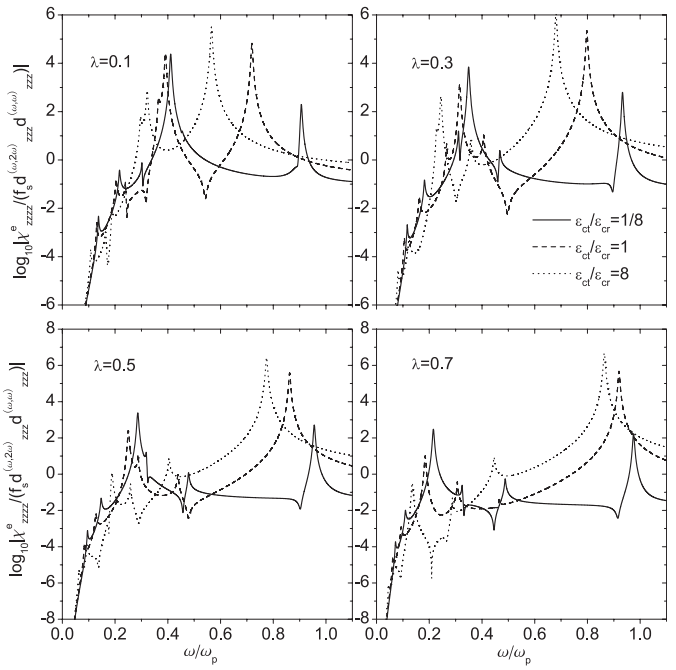

Fig. 4. Same as Figure 3, but for induced THG susceptibility $|\chi^e_{zzzz}/(f_s d^{(\omega,2\omega)}_{zzz} d^{(\omega,\omega)}_{zzz}]|$.

and correspondingly, the averages fields in the core and the shell are

$$\langle \mathbf{E}_c \rangle = A_2 E_L r_0^{\nu_2 - 1} \mathbf{e}_z \quad \text{and} \quad \langle \mathbf{E}_s \rangle = E_L B_2 \mathbf{e}_z. \tag{13}$$

As a result, we obtain the relation between $\mathbf{E}_0$ and $\mathbf{E}_L$ for Model B,

$$\mathbf{E}_L = \frac{Q_2}{Q_2 - \frac{f}{\lambda} P_2} \mathbf{E}_0. \tag{14}$$

Again, we suppose the nonlinear susceptibility for second harmonic generation of the shell $d_{lll} \neq 0$ for $l = x, y, z$ only. As consequence, the effective SHG susceptibility d^e_{zzz} and the induced THG susceptibility χ^e_{zzzz} have

$$\frac{d^e_{zzz}}{(f/\lambda - f) d_{zzz}} = (B_2^\omega)^2 B_2^{2\omega} + \frac{4\lambda}{5} \left[2 B_2^\omega C_2^\omega C_2^{2\omega} + (C_2^\omega)^2 B_2^{2\omega} \right] + \frac{8}{35} \lambda (1+\lambda) (C_2^\omega)^2 C_2^{2\omega} \tag{15}$$

and

$$\begin{aligned} \frac{\chi^{(\omega,\omega,\omega)}_{e,zzzz}}{(f/\lambda - f) d^{(\omega,2\omega)}_{zzz} d^{(\omega,\omega)}_{zzz}} &= \frac{2}{385(\epsilon_s^{2\omega} - \epsilon_{e2}^{2\omega})} \left\{ 77 (B_2^\omega)^3 \right. \\ &\times \left[5 \left(-1 + B_2^{2\omega} \right) B_2^{3\omega} + 4\lambda C_2^{2\omega} C_2^{3\omega} \right] + 132 \lambda (B_2^\omega)^2 C_2^\omega \\ &\times \left[7 B_2^{3\omega} C_2^{2\omega} - 7 C_2^{3\omega} + 7 B_2^{2\omega} C_2^{3\omega} + 2(1+\lambda) C_2^{2\omega} C_2^{3\omega} \right] \\ &+ 132 \lambda B_2^\omega (C_2^\omega)^2 \left[2 C_2^{3\omega} [(1+\lambda)(B_2^{2\omega} - 1) \right. \\ &+ 2(1 + \lambda + \lambda^2) C_2^{2\omega}] + B_2^{3\omega} (-7 + 7 B_2^{2\omega} + 2(1+\lambda) C_2^{2\omega}) \Big] \\ &+ 8 \lambda (C_2^\omega)^3 \left[2 C_2^{3\omega} [11 (1 + \lambda + \lambda^2)(B_2^{2\omega} - 1) \right. \\ &+ 10 (1 + \lambda + \lambda^2 + \lambda^3) C_2^{2\omega}] + 11 B_2^{3\omega} [(1+\lambda)(B_2^{2\omega} - 1) \\ &\left. \left. + 2(1 + \lambda + \lambda^2) C_2^{2\omega}] \right] \right\}, \end{aligned} \tag{16}$$

where $\epsilon_{e2}^{2\omega}$ has the same form as equation (10), except that P_1 (or Q_1) is replaced by P_2 (or Q_2).

In model B, we choose the same material parameters as those in Model A. For instance, the nonlinear shell is assumed to be a Drude metal, while the anisotropic core possesses frequency-independent radial dielectric constant $\epsilon_{cr} = 2.52$.

In Figures 3 and 4, the effective SHG susceptibility and the induced THG susceptibility per unit volume of nonlinear coated material are plotted as a function of frequency ω/ω_p for various ratios of tangential dielectric constant ϵ_{ct} to radial dielectric constant ϵ_{cr}. It is found that the enhancement factor of the order of 10^4 for SHG susceptibility (or 10^6 for THG susceptibility) can be achieved at several surface plasmon resonant frequencies. Actually, by tuning the core-shell geometrical ratio and/or the dielectric anisotropy of the core, the spatial local field can be enhanced which leads to large enhancement of nonlinear optical responses of the composite. To one's interest, in comparison with Figures 1 and 2, there exist four peaks for SHG susceptibility as shown in Figure 3 and six peaks for induced THG susceptibility (see Fig. 4) in Model B, which are as twice as those for model A. The reason is that the coated material is metallic and the local field in the shell is inhomogeneous for model B. As a result, two fundamental resonant frequencies ω_{c1} and ω_{c2} appear, whose difference $\omega_{c2} - \omega_{c1}$ is found to be strongly dependent on the interfacial parameter and the radially dielectric anisotropy. When the tangential dielectric constant ϵ_{ct} is decreased, the enhancement peak exhibits blue-shift, and the difference $\omega_{c2} - \omega_{c1}$ becomes large.

In the end, we show the effective SHG susceptibility as a function of frequency ω/ω_p for various λ in Figure 5.

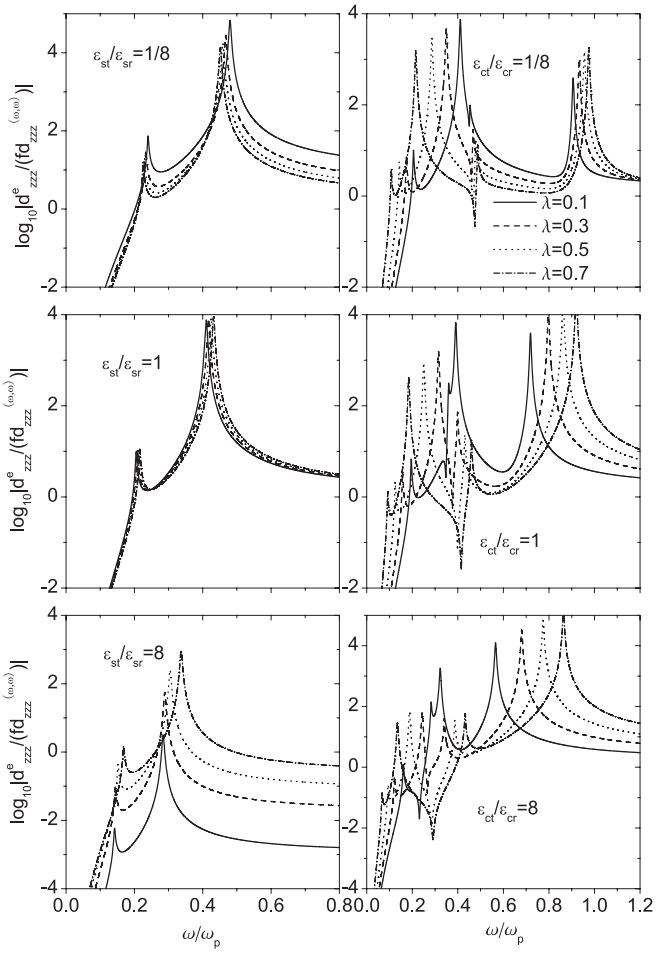

Fig. 5. $|d^{e}_{zzz}/(fd^{(\omega,\omega)}_{zzz})|$ as a function of ω/ω_p for various interfacial parameter λ and different ratios of tangential dielectric constant to radial dielectric constant. The figures on the left column are for Model A while the right ones are for Model B.

For model A, we find that when the ratio of tangential dielectric constant to radial dielectric constant is small, appreciable enhancement peaks in higher frequency region are found, and the increase of the interfacial parameter λ leads to blue-shift of the resonant frequencies. However, in the case of the large ratio of tangential dielectric constant to radial dielectric constant, increasing λ results in the red-shift of the resonant frequencies. On the other hand, the figures for Model B are more complicated than the ones for Model A. In detail, there exist two fundamental resonant frequencies due to the coating material being metallic, and four resonant peaks dominate the spectra of SHG susceptibility. Note that the enhancement peak exhibits a red-shift in low frequency region and a blue-shift in high frequency region with the increase of the interfacial parameter λ.

5 Discussion and conclusion

In this paper, we have investigated the effective nonlinear susceptibilities for second harmonic generation (SHG) and induced third harmonic generation (THG) of nonlinear composite materials, in which nondilute coated particles with radial dielectric anisotropy are embedded in the linear host. Two typical coated particles are studied. The first is that the core being second order nonlinear and the shell being radially dielectric anisotropic, while the second is the core being anisotropic and the shell being nonlinear. In both cases, we observe large enhancement of SHG and induced THG susceptibilities at several surface plasmon resonant frequencies.

It is found that the dielectric anisotropy and the core-shell structure play important roles in determining the nonlinearity enhancement and the surface resonant frequencies. And the adjustment of the dielectric anisotropy may result in large enhancement of both SHG and induced THG susceptibilities at surface plasmon resonant frequencies. For model B, we find that there exist two fundamental resonant frequencies ω_{c1} and ω_{c2} due to the coated material being metallic. In addition, the interfacial parameter can affect the nonlinear responses of the two systems. Therefore, by choosing proper interfacial parameter and radially dielectric anisotropy, we can obtain the large enhancement of SHG and induced THG susceptibilities at surface plasmon resonant frequencies.

In our paper, we have considered that the coated particles to be in the nondilute limit ($f = 0.1$). In this regard, we take into account the electrostatic dipolar interaction among the coated particles and introduced a Lorentz field $\mathbf{E}_L$ to derive our formulae for effective SHG and THG susceptibilities. In this connection, the enhancement of effective nonlinear susceptibilities in nondilute limit is found to be than the one in the dilute limit [13].

As a matter of fact, dielectric anisotropy exists in many nanostructures such as in biological cells [20] and in real phospholipid vesicles [27]. In material science, people discovered giant multiple-shell structures which called onion-like fullerences [28], whose dielectric properties possess the radial anisotropy [29]. The multishell may be filled with gold clusters and be surrounded by a third material [30], just as our Model A. In general, the dielectric response for nematic liquid crystal droplet is more complex, for its structure depends on many factors such as the interfacial interactions between the liquid crystal and the surrounding medium, temperature, and the external electric or magnetic field. The radial dielectric response may be realized for strong molecular anchoring perpendicular to the liquid-crystal-polymer interface [31]. More recently, optical properties of a subwavelength metallic ellipsoid covered by an optically anisotropic molecular layer are studied [32], in which the model is similar as our model A too. In addition, Model B may be realized by adding metallic shells to the functionally graded particles which often have the local dielectric anisotropy. We hope our theoretical predictions may help to improve the experimental investigation.

This work was supported by the National Natural Science Foundation of China for financial support under Grant No. 10674098.

References

1. G.I. Stegeman, in *Contemporary Nonlinear Optics*, edited by G.P. Agrawal, R.W. Boyd (Academic Press, Boston, 1992)
2. V.M. Shalaev, *Nonlinear Optics of Random Media: Fractal Composites and Metal-Dielectric Film* (Springer-Verlag, Berlin, 2000)
3. D. Cotter, R.J. Manning, K.J. Blow, A.D. Ellis, A.E. Kelly, D. Nesset, I.D. Phillips, A.J. Poustie, D.C. Rogers, Science **286**, 1523 (1999)
4. D. Stroud, V.E. Wood, J. Opt. Soc. Am. B **6**, 778 (1989)
5. O. Levy, D.J. Bergman, D. Stroud, Phys. Rev. E **52**, 3184 (1995)
6. D.J. Bergman, O. Levy, D. Stroud, Phys. Rev. B **49**, 129 (1994)
7. L. Gao, L.P. Gu, Z.Y. Li, Phys. Rev. E **68**, 066601 (2003)
8. P.M. Hui, Phys. Rev. B **49**, 15344 (1994)
9. G.L. Fisher, R.W. Boyd, R.J. Gehr, S.A. Jenekhe, J.A. Osaheni, J.E. Sipe, L.A. Weller-Brophy, Phys. Rev. Lett. **74**, 1871 (1995)
10. K. Mallik, M. Mandal, N. Pradhan, T. Pal, Nano. Lett. **1**, 319 (2001)
11. J.J. Schneider, Adv. Mater. **13**, 529 (2001)
12. A.E. Neeves, M.H. Birnboim, J. Opt. Soc. Am. B **6**, 787 (1989)
13. P.M. Hui, C. Xu, D. Stroud, Phys. Rev. B **69**, 014203 (2004)
14. L. Gao, Phys. Lett. A **318**, 119 (2003)
15. Y. Yang, M. Hori, T. Hayakawa, M. Nogami, Surf. Sci. **579**, 215 (2005)
16. G.W. Lu, B.L. Cheng, H. Shen, Y.J. Chen, T.H. Wang, Z.H. Chen, H.B. Lu, K.J. Jin, Y.L. Zhou, G.Z. Yang, Chem. Phys. Lett. **579**, 397 (2005)
17. K.P. Yuen, M.F. Law, K.W. Yu, Ping Sheng, Phys. Rev. E **56**, R1322 (1997)
18. A.A. Lucas, L. Henrard, Ph. Lambin, Phys. Rev. B **49**, 2888 (1994)
19. J.C.E. Sten, IEEE Trans. Dielectrics and Electrical Insulation **2**, 360 (1995)
20. V.L. Sukhorukov, G. Meedt, M. Kurschner, U. Zimmermann, J. Electrostat. **50**, 191 (2001)
21. P.M. Hui, D. Stroud, J. Appl. Phys. **82**, 4740 (1997)
22. P.M. Hui, P. Cheng, D. Stroud, J. Appl. Phys. **84**, 3451 (1998)
23. L. Gao, K.W. Yu, Phys. Rev. B **72**, 075111 (2005)
24. L. Gao, Phys. Rev. E **71**, 067601 (2005)
25. J.I. Dadap, J. Shan, K.B. Eisenthal, T.F. Heinz, Phys. Rev. Lett. **83**, 4045 (1999)
26. N. Yang, W.E. Angerer, A.G. Yodh, Phys. Rev. Lett. **87**, 103902 (2001)
27. B. Lange, S.R. Aragon, J. Chem. Phys. **92**, 4643 (1990)
28. D. Ugarte, Nature **359**, 707 (1992)
29. A.A. Lucas, L. Henrard, Ph. Lambin, Phys. Rev. B. **49**, 2888 (1993)
30. D. Ugarte, Chem. Phys. Lett. **209**, 99 (1993)
31. I. Vilfan, M. Vilfan, S. Zumer, Phys. Rev. A. **40**, 4724 (1989)
32. T. Ambjornsson, Phys. Rev. B. **73**, 085412 (2006)